IEEE Open Journal of Nanotechnology

Received 4 July 2020; revised 31 July 2020 and 22 August 2020; accepted 22 August 2020. Date of publication 25 August 2020; date of current version 12 November 2020. The review of this paper was arranged by Associate Editor Yunlong Zi.

Digital Object Identifier 10.1109/OJNANO.2020.3019425

Stretchable Triboelectric Nanogenerators for Energy Harvesting and Motion Monitoring

JIAHUI HE, YIMING LIU, DENGFENG LI, KUANMING YAO, ZHAN GAO, AND XINGE YU

Department of Biomedical Engineering, City University of Hong Kong, Hong Kong 999077, China

CORRESPONDING AUTHOR: XINGE YU (e-mail: xingeyu@cityu.edu.hk)

This work was supported by City University of Hong Kong under Grants 9610423 and 9667199, Research Grants Council of the Hong Kong Special Administrative Region under Grant 21210820, and Science and Technology of Sichuan Province under Grant 2020YFH0181. Jiahui He and Yiming Li contributed equally to this article.

This article has supplementary downloadable material available at https://ieeexplore.ieee.org, provided by the authors.

ABSTRACT Motion monitoring by flexible strain or pressure sensors have been under spotlight in the field of wearable electronics. Based on triboelectric effect, generated energy from body contact and compression during daily movement can be used for both reflecting motion status and energy recollection. Here, we report a stretchable pressure sensor based on triboelectric effect and dots-distributed metallic electrodes, adopting contact-separation mode. The dots-distributed electrode based triboelectric nanogenerator (D-TENG) could be easily integrated with body and cloth, such as on the skin and under foot, to sense a broad range of activity related strain information. The D-TENGs enable accurate detecting a broad range pressure from ∼5 kPa to ∼50 kPa with open circuit voltage variation from several volts to tens of volts, and thus allow monitoring body daily actives such as joints' bending, walking and running. These devices maintain stable and high-level signal outputs even after thousands cycles of measurement, proving the good stability. Simultaneously, the mechanical energy produced by our body motions could also be recollected by the D-TENG sensor for energy harvesting. Under a constant tapping by finger (39.59 kPa), the induced voltage is sufficient to light up 15 LEDs. The stretchable D-TENG sensor indicates its great potential in motion monitoring and mechanical energy harvesting.

INDEX TERMS Energy harvesting, motion monitoring, stretchable electronics, strain sensors, triboelectric nanogenerators.

I. INTRODUCTION

The great applications of wearable electronics, such as healthcare [1]–[6], human-machine interface [7], [8] and motion recognition [9]–[11], have attracted much attention over the past decades. Compared to the traditional electronics based on rigid and brittle Si platform, flexible electronics exhibit great deformability and excellent electrical properties [12]. In recent years, intrinsically stretchable/flexible materials [13]–[17] and fancy structural mechanics designs, i.e. serpentine [18], [19], island-bridge [19], [20], and nano-mesh [21], [22], have been adopted to develop various kinds of flexible devices for monitoring humidity [23], temperature [24], [25], pressure and human motion [26]–[29]. To fully realized the advantage, bulky parts such as batteries are needed to be replaced by thin, soft self-power components. To date, self-power technologies based on thermoelectric [30], [31], optical effects [32], [33] piezoelectric[34]–[36], and triboelectric effects have been developed [37]–[40]. Among them, triboelectric nanogenerators (TENGs) are good candidates as which can not only serve as energy harvesters but also act as self-powered sensors. TENGs can generate considerable electricity through contact-separation at the interface of two materials surface with different electrical natures [41], [42]. The human body motion induced contact-separations between skin and device could be used for motion monitoring as well as a platform for mechanical energy harvesting [43], [44].

TENG-based sensors include single-electrode mode and contact-separation mode, where single-electrode mode TENGs take advantage of simple structure and fabrication: only one triboelectric layer coupling with a conductive layer is required in a device. Given above, this laboratory has reported filmy, skin-integrated TENGs combing single-electrode mode

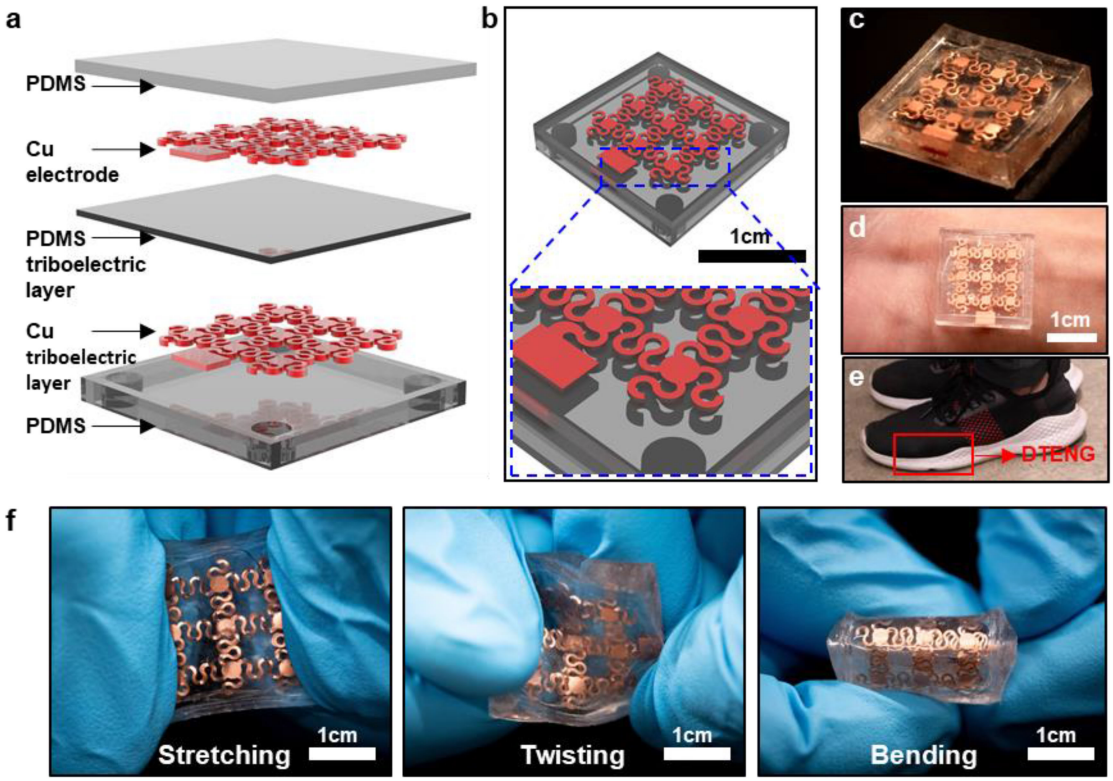

FIGURE 1. **Schematic diagram of a dots-distributed electrode-based triboelectric nanogenerator (D-TENG). (a) The schematic illustration of a D-TENG. (b) The stretchable electrode patterns. (c) Optical image of the D-TENG on the desk and (d) on human skin. (e) The D-TENG is tiny enough to be fitted into a shoe. (f) Optical image of the D-TENG under stretching, twisting, and bending.**

and structural mechanics design [28], [45]. Nevertheless, the performance of single-electrode mode TENGs would vary when contact with different objects, or work under different humidity [45], limiting their practicability in accurate pressure sensing and stable power supplying. In contrast, the couple of functional triboelectric layers are encapsulated in a contact-separation mode TENGs, averting the above problem. Besides, metallic thin film, silver nanowire networks [27], [46], carbon nanotubes [47] and graphene [48] are the mostly used electrodes for TENGs. Metallic thin film electrodes (gold or copper) present great and stable electrical conductivity that is very suitable for a conductive layer as well as a proper passive triboelectric layer. Given the above, combing the stretchable layout of electrode with contact-separation mode TENG still need further study.

Here we report a contact-separation mode TENG sensors based on copper electrode with dots-distributed layout. Copper electrode and PDMS serve as positive and negative triboelectric layers, respectively. The sensors present great sensitivity and stability under a broad range of strains/pressures. With the serpentine electrode patterns, the D-TENG exhibit great flexibility and durability under various mechanical situations such as large-angle bending, twisting and stretching, maintaining stable signal output even after thousands cycles of finger beating with pressure of 17∼22 kPa. Moreover, body motion induced high output voltage of the D-TENG sensor would be a good source for energy harvesting and self-power wearable device. These contact-separation mode D-TENGs show a great potential in energy harvesting and stable motion monitoring.

II. MATERIALS AND METHODS

The D-TENG sensor adopt a symmetric structure with multiply layer stacking layouts, consisting of three layers of PDMS and two layers of copper thin film electrode. As shown in Fig. 1(a), the top and bottom PDMS layers both serve as the substrates and encapsulation layers with same thickness. To ensure good adhesion and stretchability, PDMS (Sylgard 184, Dow Corning Corporation) was prepared by the proportional cross-link agent and per-polymer of 1:20. The molds used for PDMS layers formation were realized by 3D printing. The proportioned PDMS was poured into the molds, vacuumed for 20 min to remove air bubbles, then cured in an oven at 40 °C for 5 h. Peeling off the PDMS from the molds formed two substrate PDMS layers. One layer is sized of 2 cm × 2 cm × 2 mm and the other contains a 2 cm × 2 cm × 2 mm substrate and four surrounded 1.1 mm-height ×1 mm-width walls. The device can be adhered on the skin with either sides.

The middle 88- μm-thick PDMS film serves as negative triboelectric layer. With a layer of stretchable 6- μm-thick copper electrode, the negative triboelectric PDMS layer was bonded on the top PDMS substrate. The stretchable copper

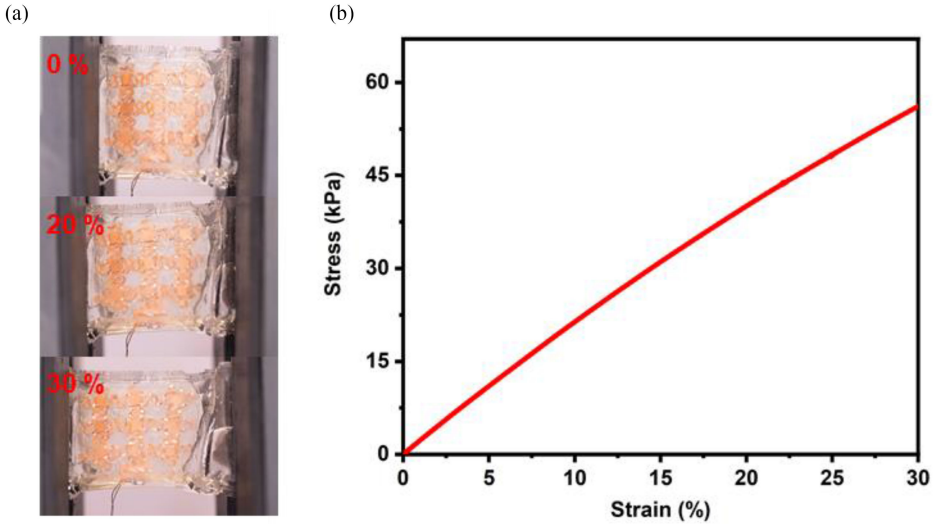

FIGURE 2. The tensile test of D-TENG. (a) Optical images of the D-TENG under strain of 0%, 20% and 30%. (b) The stress-strain curve of D-TENG under strain from 0% to 30%.

electrode was prepared as follows. A piece of 6- μm-thick copper foil was flattened by a cylinder on a glass substrate with a very thin PDMS layer. Then, AZ 4620 photoresist (AZ Electronic Materials) was spin-coated on copper foil at 3000 rpm for 30 s and soft baked at 115 °C for 5 min. With designed mask, the sample was exposed under a mask aligner (URE-2000/35AL deep UV, IOE, CAS) for 45 s. After developing in AZ 400K developer and post-bake for 5 min at 115 °C, the patterned copper foil was wet etched in FeCl3 solution. Thus, the stretchable copper electrode was realized. Then, after cleaning the copper electrode by acetone, PDMS precursor (crosslink agent: per-polymer = 1:10) was spin-coated on the electrode at 1300 rpm for 30s to form an 88- μm-thick PDMS layer as the negative triboelectric layer. With un-crosslinked PDMS and subsequent curing process, the 88- μm PDMS layer with electrode could be tightly attached on the top substrate and leaving the triboelectric layer facing down.

With the same method, we fabricated another stretchable copper electrode on the bottom PDMS substrate with exposed electrode facing up. Finally, the top and bottom substrate were adhered together using PDMS adhesive layer to ensure the entire device encapsulated well. By then, the D-TENG device was completed. It works by the contact-separation mode between 88- μm PDMS negative triboelectric layer and bottom positive triboelectric layer (stretchable 6- μm copper electrode). The output voltage and current can be derived from both the top and bottom electrodes.

The tensile test was carried out using a mechanical testing system (INSTRON 5942 Testing System) with an elongation speed of 10 mm min−1 at room temperature. The sample was a complete D-TENG with extra length for clamping. To test the influence of the thickness of PDMS negative triboelectric on the D-TENG performance, we fabricated a series of PDMS thin layer with different thicknesses. The thickness was measured by optical surface profiler (Veeco/Wyko NT9300). The open-circuit voltage of the D-TENGs was measured by a DAQ multimeter (Keithley 6510) at a sampling rate of 60 kHz. The short-circuit current of the D-TENGs was calculated by measuring the voltage of a resistor connecting in series with the D-TENG (through PL3516/P Powerlab 16/35, AD Instruments, at a sampling rate of 10 kHz). The current could be calculated according to the voltage and resistance. The D-TENG was operated and tested on a volunteer body with his full and informed consent.

III. RESULTS AND DISCUSSION

To develop a stable and stretchable device for motion monitoring, we combine TENG effect and mechanics design together to fabricate a contact-separation mode TENG sensor with two dots-distributed electrodes. Fig. 1(a) illustrates the schematic diagram of the dots-distributed electrode-based triboelectric nanogenerator (D-TENG) sensor. To increase the stretchability of this sensor, we design the 6- μm-thick copper electrodes with distributed dots connected by thin serpentines (Fig. 1(b)), that ensures a large voltage output as well as good stretchability. This sensor works through the contact-separation process between middle 88- μm-thick PDMS negative triboelectric layer and bottom stretchable 6- μm copper electrode as positive triboelectric layer, due to their corresponding electrical negative and positive nature [49], [50]. The induced signals including voltage and current are derived from both the top and bottom electrodes.

To realize the contact-separation process, the middle PDMS layer with electrode is tightly attached on the top substrate with triboelectric layer facing down. Another stretchable copper electrode is on the bottom PDMS substrate with exposed electrode facing up. The gap between them is about 1.1 mm. We realize this fixed gap by utilizing two 3D printed molds. After assembling the top and bottom parts, the device with size of 2 cm × 2 cm × 4.5 mm is obtained, as shown in

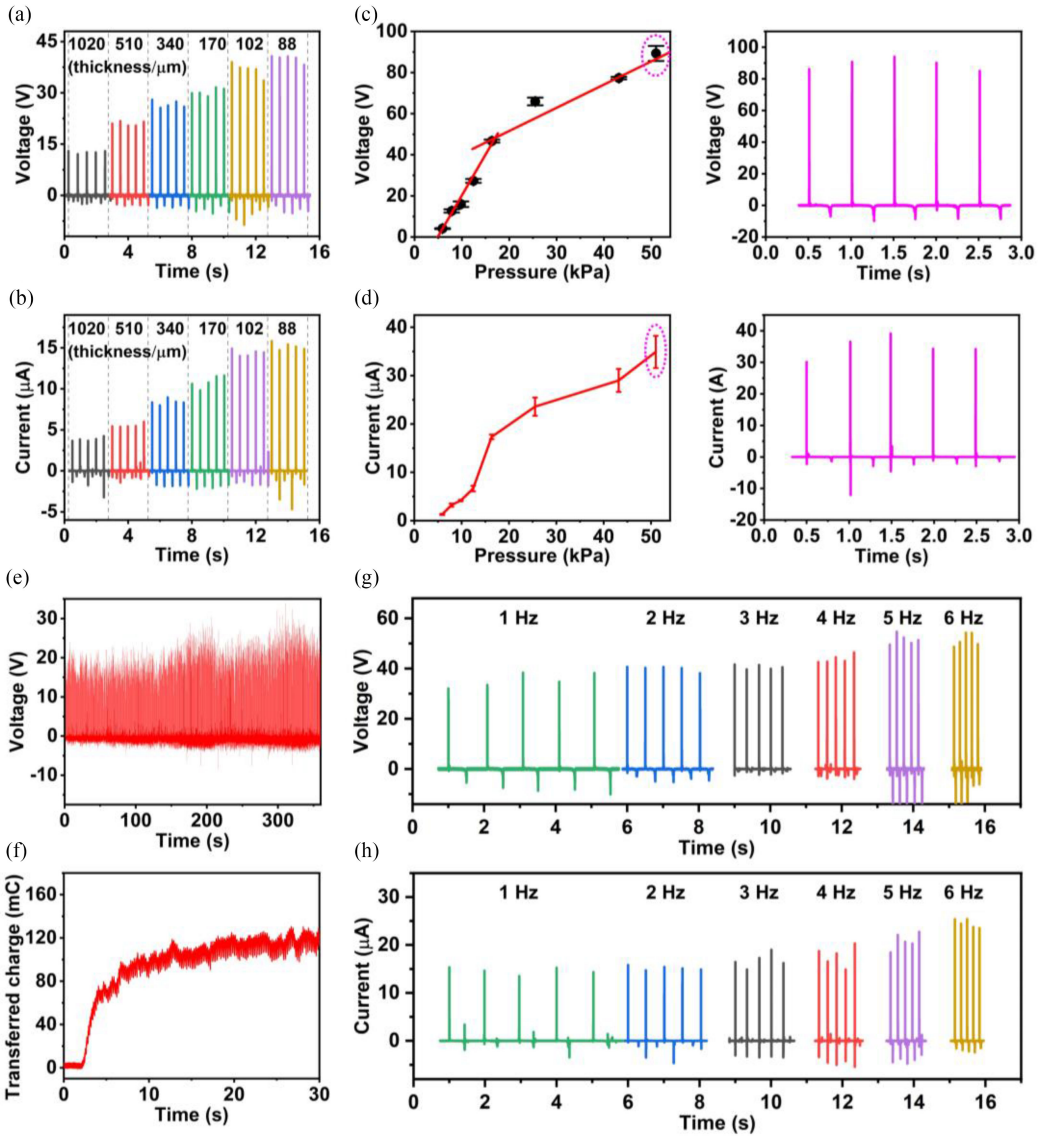

FIGURE 3. **Electrical performances of the D-TENG sensor. (a) The open-circuit voltage and (b) short-circuit current by D-TENG as a function of PDMS triboelectric layer thickness under constant pressure of 15.03 kPa and frequency of 2 Hz. (c) The open-circuit voltage and (d) short-circuit current by D-TENG as a function of pressure under a frequency of 2 Hz. (e) The stability of D-TENG at constant pressure of 17∼22 kPa and frequency of 4 Hz for 1440 cycles. (f) The transferred charge for capacitors with 0.1 μF after rectification by full-wave bridge rectifier, under a constant pressure of 45.23 kPa at frequency of 5 Hz. (g) The open-circuit voltage and (h) short-circuit current by D-TENG as a function of frequency under constant pressure of 14.77 kPa.**

Fig. 1(c). The entire device is encapsulated by PDMS substrate to prevent the corrosion and oxidation of electrodes, caused by sweat, oxygen and vapour. The minimum width line of electrode pattern is 400 μm, the weight of an as-fabricated D-TENG sensor is 1.54 g. Such light device is very portable. Actually, both sides of the sensor can be easily and nonirritatingly attached on human skin by the low modulus PDMS (1:20) interfaces (Fig. 1(d)). For further motion monitoring and energy harvesting, we also integrated the D-TENG sensor into a shoe, as demonstrated in Fig. 1(e).

Fig. 1(f) presents that the D-TENG sensor owns good flexibility and stretchability. PDMS has already been commonly used in flexible electronics for its good physical/chemical stability and flexibility [51]. The substrates with soft 1:20 PDMS allows the high degree deformation. The design of dots-distributed electrode associate with arrayed separated square electrodes connecting by serpentines traces, offering the Cu electrode good stretchability and flexibility. The separated square electrodes are designed to increase the contact area of the triboelectric surfaces, which will enhance the electrostatic induction between triboelectric layer and electrode, and magnify the triboelectric performance [52]. As shown in Fig. 1(f), the electrodes and device still remain robust even under 25% strain, twisting and 180 degrees bending. In addition, a tensile test was carried out to furtherly exhibit its great stretchability, as shown in Fig. 2. Under an increasing uniaxial

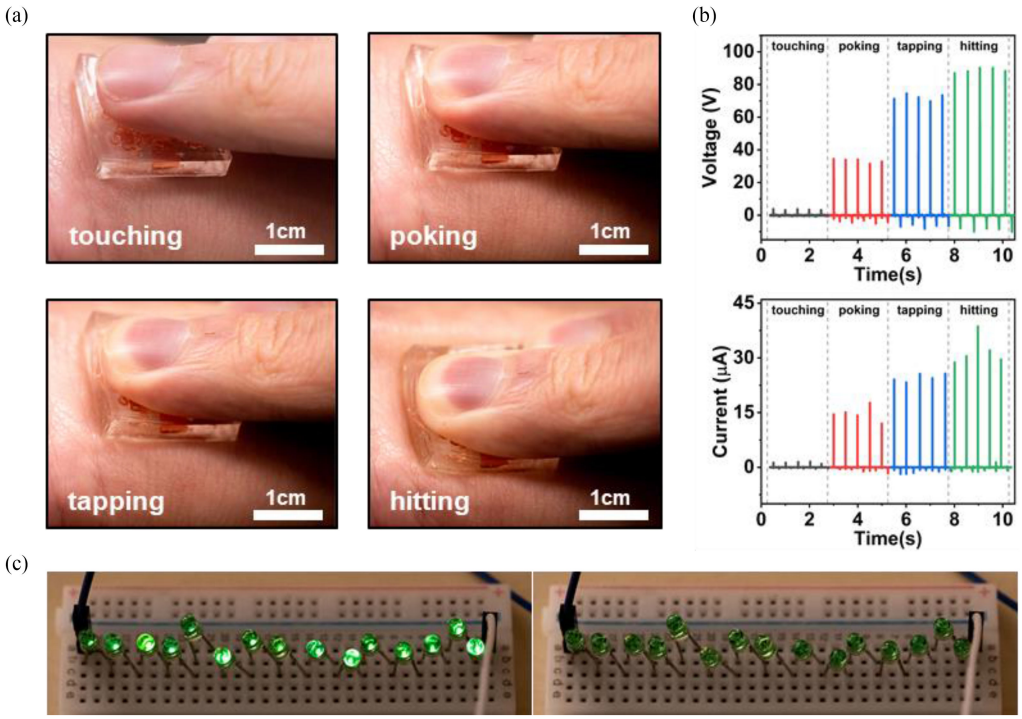

FIGURE 4. D-TENG sensor on the skin for pressure sensing and energy harvesting. (a) Optical images showing four different external loads, named touching, poking, tapping, and hitting, by a finger on the D-TENG. The sensor is attached on the skin (b) The open-circuit voltage and short-circuit current by D-TENG under different loads. (c) 15 LEDs were lighted up by the D-TENG under fingers beating.

strain from 0% to 30%, the original length (20 mm) of the device was lengthened to 26 mm, however, there was no any visible crack on the entire structure (Fig. 2(a)); meanwhile, the stress-strain curve (Fig. 2(b)) presents quite low stress even under high-level strain, indicating its successful mechanics design and good portability.

We select the 1:10 PDMS to fabricate the triboelectric layer of D-TENG. Its stiffness can achieve good triboelectric performances with proper stretchability. Meanwhile, the surface is less sticking to ensure the good separation ability during contact-separation process. In a contact-separation process driven by constant pressing, the electrons would inject from the copper electrode to the PDMS; when the D-TENG is released, the PDMS surface separates away from the button copper electrode, leaving a potential difference between the couple of electrodes, and the induced electrons would flow from negative side to positive side, as shown in Fig. 1. Based on above working principle, the D-TENG could transfer mechanical energy into electricity. To study the influence of triboelectric layer's thickness on the device electrical performance, we fabricated the devices with different thick middle PDMS layers. By adjusting the spin-coating rpm, the middle PDMS layer with thickness of 1.02mm, 510 μm, 340 μm, 170 μm, 102 μm and 88 μm were fabricated. The thickness was measured by optical surface profiler (Veeco/Wyko NT9300). Fig. 3(a) and b exhibits the open-circuit voltage and short-circuit current as functions of a series of PDMS thickness. Under external pressure of 15.03 kPa at 2 Hz, the output signal of D-TENG increased obviously with the decrease of PDMS layer thickness. For thickness of 1.02 mm, open-circuit voltage and short-circuit current are 12.61 $\pm$ 0.35 V and 3.75 $\pm$ 0.32 μA, respectively. When the thickness decreases to 88 μm, the corresponding peak values of open-circuit voltage and short-circuit current are up to 39.7 $\pm$ 1.17 V and of 15.2 $\pm$ 0.44 μA. The result indicates that the thinner triboelectric layer would perform better electrical signals by enhancing the electrostatic induction between the electrode and triboelectric layer. However, considering the triboelectric performance and device stability, the 88 μm in this work is an optimized value. [53], [54]**.** Therefore, the D-TENG with 88 μm PDMS triboelectric layer was selected as a representative sample for the following test.

Generally, larger pressure induces stronger triboelectric effect. Fig. 3(c), d shows the open-circuit voltage and short-circuit current as functions of external pressure at a constant frequency of 2 Hz. Obviously, both the voltage and current increased as the external pressure rises. Moreover, the output signal is also outstanding with 4.09 $\pm$ 0.24 V voltage and 1.31 $\pm$ 0.12 μA current under only 5.9 kPa, which enables the sensing of small pressure. Then, the voltage and current signals increase to 88.7 $\pm$ 1.42 V and 34.9 $\pm$ 3.33 μA under large pressure of 50.98 kPa. In details, the measured value of open-circuit voltage was quite considerable and highly sensitive among the applied pressure, the sensitivity were 3.97 $\pm$ 0.17 mV/Pa ($<$ 17.03 kPa) and 1.13 $\pm$ 0.11 mV/Pa ($>$ 17.03 kPa) respectively, for which the device can be used

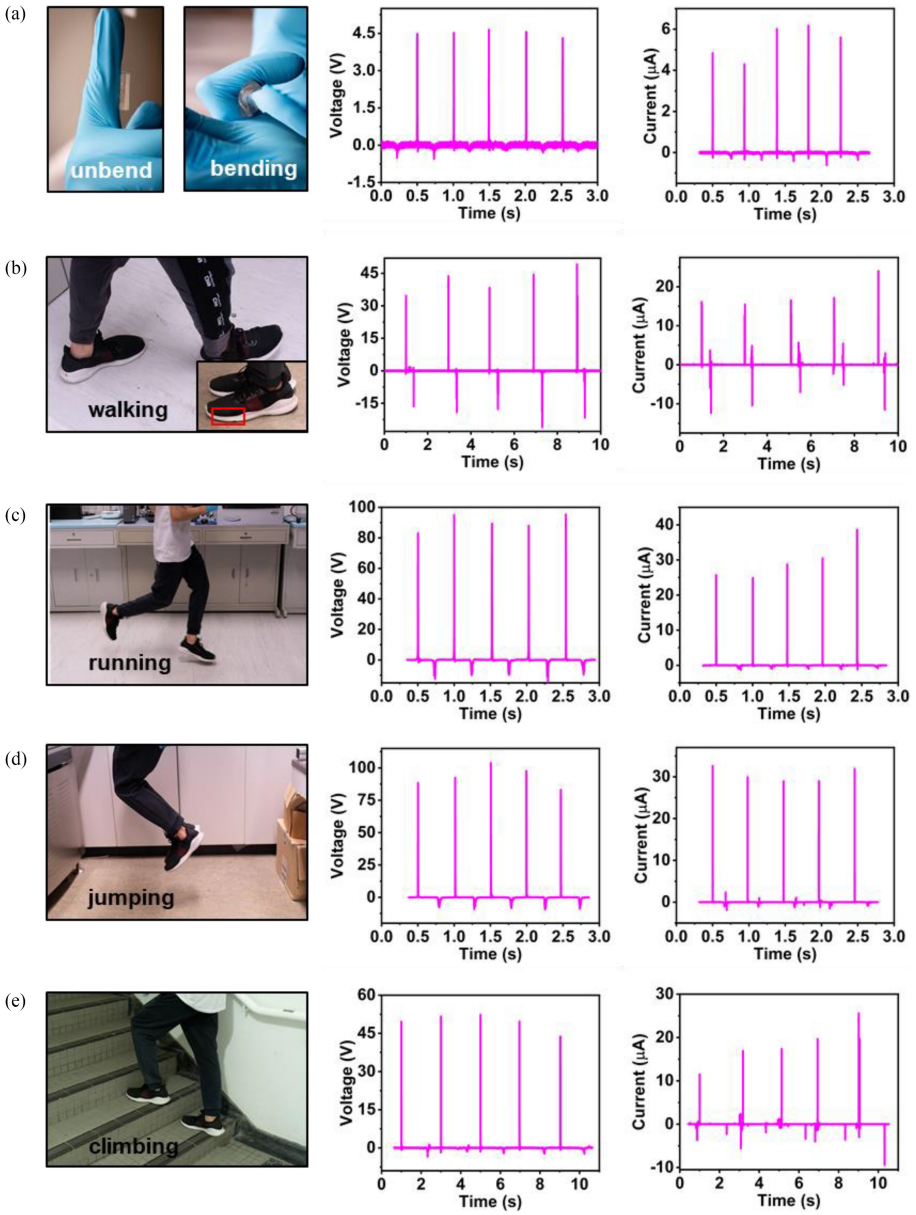

FIGURE 5. **D-TENG sensors for motion monitoring. Optical images and the corresponding output signals for different body motions. (a) finger joint bending, (b) walking, (c) running, (d) jumping, and (e) climbing.**

for pressure sensing without any additional amplifiers. The waveforms of the signal under the 50.98 kPa pressure are shown in the right side of Fig. 3(c) and d. The signals amplitude keeps uniform under such large pressure, indicating that the D-TENG remains pretty good performances and the triboelectric layers also achieve good contact and separation.

Besides, to test the stability of the D-TENG in practical application, a constant pressure about 17 $\sim$ 22 kPa at a frequency of 4 Hz was applied on the device for 6min by human finger beating. As shown in the Fig. 3(e), the output signal generated from the D-TENG was quite stable during 1440 cycles, about 16 $\sim$ 27 V, which proves the ruggedness of the device structure.

In addition, the charging performance test of the device for 0.1 μF capacitance was carried out in a rectified circuit, as shown in Fig. S2. When a capacitor was connected to the circuit, the charge generated from the device transferred to the capacitor. As shown in Fig. 3(f), by constantly tapping the device with a pressure of 45.13 $\pm$ 1.42 kPa at frequency of 5 Hz, the capacitor reached up to 100 mC within 20 s.

The electrical performances of D-TENG under constant pressure of 14.77 kPa at frequencies of 1 Hz, 2 Hz, 3 Hz, 4 Hz, 5 Hz and 6 Hz were also demonstrated in Figs. 3(g) and (h). Even though the frequency varied, both the open-circuit voltage and short-circuit current changes a little. The specific values are 35.37 $\pm$ 2.9 V, 40.04 $\pm$ 1.04 V, 40.53 $\pm$

0.98 V, 43.92 ± 1.61 V, 51.68 ± 2.03 V, 51.50 ± 2.66 V and 14.65 ± 0.74 μA, 15.21 ± 0.44 μA, 16.79 ± 1.52 μA, 17.76 ± 2.08 μA, 20.88 ± 1.68 μA, 24.52 ± 0.9 μA. The slightly signal increase may result from the increasing inductive impedance of DAQ multimeter with the increasing frequency of AC signal. By the way, the signal interval is always corresponding to the frequency of the applied force, indicating that the D-TENG owns good responsiveness even under high-frequency external pressure. Overall, the results under high external force, high-frequency beating or long-time operating shows good response and stability of D-TENG, exhibiting its realizable potential in pressure sensor, body motions monitoring and wearable energy harvesting in daily life.

Integrated on the skin, the D-TENG sensor can realize various pressure sensing as a wearable device. We applied four kinds of different external pressure loads, named touching, poking, tapping, and hitting, on the sensor to estimate its practical performance (Fig. 4(a)). Attached on a volunteer's wrist, the sensor was touched, poked, tapped and hit by human fingers at the frequency of 2 Hz. The responding pressures are 4.5 ± 1.58 kPa, 15.08 kPa ± 2.12 kPa, 39.59kPa ± 1.87 kPa and 53.8 ± 2.91 kPa, respectively. The Fig. 4(b) shows that values of the output signals increase with the loaded pressure rising. For general slight touching, the open-circuit voltage and short-circuit current reached 3.47 ± 0.32 V and 1.32 ± 0.23 μA, respectively, which proves that the pressure sensor is quite sensitive for the pressure sensing. When heavily hitting the sensor, the corresponding values boosted up to 88.75 ± 1.42 V and 31.91 ± 3.96 μA. Therefore, the D-TENG sensor shows a very wide range of pressure sensing. Besides pressure sensing, the generated electrical signal could also be recollected for energy harvesting. Fig. 4(c) demonstrates that 15 LEDs were lighted up by a D-TENG sensor in a rectified circuit (Fig. S2) under the tapping of a finger (∼37 kPa, Movie S1). Therefore, during pressure sensing, the D-TENG sensor is also playing a role in energy conversion and storage. The output voltages would also be a good source for the self-power wearable devices.

Physical motion of the human body commonly includes joints movement and overall body movement. To further demonstrate the potential application of D-TENG in motion monitoring, we integrated the sensors on the finger joints or into the shoes for pressure sensing, as shown in Fig. 5. For example, when the finger bends, the mounted D-TENG will generates the contact-separation process (Fig. 5(a)). For 120 degree bending at 2 Hz, the open-circuit voltage and short-circuit current reached 4.5 ± 0.12 V and 5.39 ± 0.79 μA, respectively. On the finger, the D-TENG sensor presents good flexibility.

For actual excise, the overall body often continues to rise and fall. When body falls, the potential energy will do a lot of work, which is much greater than the kinetic energy of the joint. As shown in Figs. 5(b-e), the D-TENG sensor was mounted on the insole. During a volunteer's motion of walking (∼16.7 kPa), running (∼50.8 kPa), jumping (∼58.4 kPa) and climbing (∼18.4 kPa), the corresponding voltage and current were 42.09 ± 5.62 V, 90.14 ± 5.16 V, 93.12 ± 8.04 V, 49.42 ± 3.36 V and 17.87 ± 3.51μA, 29.7 ± 5.49 μA, 30.47 ± 1.71 μA, 20.43 ± 1.78 μA. Walking and climbing shows comparable signal output. Similarly, the values of output voltages for running and jumping is similar. Overall, the values of output signal are related to the potential energy of the motions. The results indicate the TENG devices can be used for various kind of activity monitoring, such as sensing of joint motions, steps, postures, and many others.

More importantly, the detected output signal is considerable enough for directly recording without any amplification. The good mechanical performance, stable and outstanding electrical output is quite suitable for continuous motion monitoring. Through the above practical application testing, the excellent potentials of D-TENG in motion monitoring and power charging application are well exhibited.

IV. CONCLUSION

In conclusion, we developed a soft, stretchable triboelectric nanogenerator working by contact-separation mode for energy harvesting and motion monitoring. The mechanical design of dots-distributed electrode endows the sensor good stretchability. By simple fabrication process, the acquired sensors could be integrated on the skin for pressure sensing with striking signal output. The sensing covers a wide pressure range from slight touching to heavy hitting. Moreover, after 1440 cycles, the sensor still shows stable high signal output. For general excise, the sensor mounted on the shoes could record the motion including walking, running, jumping, and climbing. Along with the motion monitoring, the generated high voltages can also light up 15 LEDs easily. This D-TENG sensor, as a wearable device, shows its outstanding performance in energy harvesting and motion monitoring, which indicates its quite realizable prospects in the broad applications of wearable devices.

REFERENCES

[1] K. Lee *et al.*, "Mechano-acoustic sensing of physiological processes and body motions via a soft wireless device placed at the suprasternal notch," *Nature Biomed. Eng.*, vol. 4, no. 2, pp. 148–158, Feb. 1, 2020.

[2] H. Wu, W. Gao, and Z. Yin, "Materials, devices and systems of soft bioelectronics for precision therapy," *Adv. Healthcare Mat.*, vol. 6, no. 10, 2017, Art. no. 1700017.

[3] Y. Liu *et al.*, "Epidermal electronics for respiration monitoring via thermo-sensitive measuring," *Mat. Today Phys.*, vol. 13, Jun. 1, 2020, Art. no. 100199.

[4] S. Choi, H. Lee, R. Ghaffari, T. Hyeon, and D.-H. Kim, "Recent advances in flexible and stretchable bio-electronic devices integrated with nanomaterials," *Adv. Mat.*, vol. 28, no. 22, pp. 4203–4218, 2016.

[5] W. Gao *et al.*, "Fully integrated wearable sensor arrays for multiplexed in situ perspiration analysis," *Nature*, vol. 529, no. 7587, pp. 509–514, Jan. 1, 2016.

[6] Y. Khan, A. E. Ostfeld, C. M. Lochner, A. Pierre, and A. C. Arias, "Monitoring of vital signs with flexible and wearable medical devices," *Adv. Mat.*, vol. 28, no. 22, pp. 4373–4395, 2016.

[7] X. Yu *et al.*, "Skin-integrated wireless haptic interfaces for virtual and augmented reality," *Nature*, vol. 575, no. 7783, pp. 473–479, Nov., 2019.

[8] M. S. White *et al.*, "Ultrathin, highly flexible and stretchable PLEDs," *Nature Photonics*, vol. 7, no. 10, pp. 811–816, Oct. 1, 2013.

[9] G. Ge *et al.*, "Stretchable, transparent, and self-patterned hydrogel-based pressure sensor for human motions detection," *Adv. Functional Mat.*, vol. 28, no. 32, 2018, Art. no. 1802576.

[10] L. Guan, S. Yan, X. Liu, X. Li, and G. Gao, "Wearable strain sensors based on casein-driven tough, adhesive and anti-freezing hydrogels for monitoring human-motion," *J. Mat. Chem. B*, vol. 7, no. 34, pp. 5230–5236, 2019.

[11] W. Guo *et al.*, "Matrix-independent highly conductive composites for electrodes and interconnects in stretchable electronics," *ACS Appl. Mat. Interfaces*, vol. 11, no. 8, pp. 8567–8575, Feb. 27, 2019.

[12] M. Mehrali *et al.*, "Blending electronics with the human body: A pathway toward a cybernetic future," *Adv. Sci.*, vol. 5, no. 10, 2018, Art. no. 1700931.

[13] S. Choi *et al.*, "Highly conductive, stretchable and biocompatible Ag–Au core–sheath nanowire composite for wearable and implantable bioelectronics," *Nature Nanotechnol.*, vol. 13, no. 11, pp. 1048–1056, Nov. 1, 2018.

[14] Y. Kim *et al.*, "Stretchable nanoparticle conductors with self-organized conductive pathways," *Nature*, vol. 500, no. 7460, pp. 59–63, Oct. 1, 2013.

[15] N. Matsuhisa *et al.*, "Printable elastic conductors with a high conductivity for electronic textile applications," *Nature Commun.*, vol. 6, no. 1, Jun. 25, 2015, Art. no. 7461.

[16] Y. Song *et al.*, "Highly compressible integrated supercapacitor–piezoresistance-sensor system with CNT–PDMS sponge for health monitoring," *Small*, vol. 13, no. 39, 2017, Art. no. 1702091.

[17] S. Zhang *et al.*, "Highly conductive, flexible and stretchable conductors based on fractal silver nanostructures," *J. Mat. Chem. C*, vol. 6, no. 15, pp. 3999–4006, 2018.

[18] K.-I. Jang *et al.*, "Soft network composite materials with deterministic and bio-inspired designs," *Nature Commun.*, vol. 6, no. 1, Mar. 13, 2015, Art. no. 6566.

[19] S. Xu *et al.*, "Stretchable batteries with self-similar serpentine interconnects and integrated wireless recharging systems," *Nature Commun.*, vol. 4, no. 1, Feb. 26, 2013, Art. no. 1543.

[20] C. Wang *et al.*, "Monitoring of the central blood pressure waveform via a conformal ultrasonic device," *Nature Biomed. Eng.*, vol. 2, no. 9, pp. 687–695, Sep. 1, 2018.

[21] M. Gong *et al.*, "Flexible breathable nanomesh electronic devices for on-demand therapy," *Adv. Functional Mat.*, vol. 29, no. 26, 2019, Art. no. 1902127.

[22] A. Miyamoto *et al.*, "Inflammation-free, gas-permeable, lightweight, stretchable on-skin electronics with nanomeshes," *Nature Nanotechnol.*, vol. 12, no. 9, pp. 907–913, Sep. 1, 2017.

[23] J. Yang, R. Shi, Z. Lou, R. Chai, K. Jiang, and G. Shen, "Flexible smart noncontact control systems with ultrasensitive humidity sensors," *Small*, vol. 15, no. 38, 2019, Art. no. 1902801.

[24] S.-K. Kang *et al.*, "Bioresorbable silicon electronic sensors for the brain," *Nature*, vol. 530, no. 7588, pp. 71–76, Feb. 1, 2016.

[25] N. Matsuhisa *et al.*, "Printable elastic conductors by in situ formation of silver nanoparticles from silver flakes," *Nature Mat.*, vol. 16, no. 8, pp. 834–840, Aug. 1, 2017.

[26] Q. Hua *et al.*, "Skin-inspired highly stretchable and conformable matrix networks for multifunctional sensing," *Nature Commun.*, vol. 9, no. 1, 2018, Art. no. 244.

[27] H. Kang *et al.*, "Fingerprint-inspired conducting hierarchical wrinkles for energy-harvesting E-skin," *Adv. Functional Mat.*, vol. 29, no. 43, 2019, Art. no. 1903580.

[28] Y. Liu *et al.*, "Thin, skin-integrated, stretchable triboelectric nanogenerators for tactile sensing," *Adv. Electron. Mat.*, vol. 6, no. 1, 2020, Art. no. 1901174.

[29] T. Yang *et al.*, "A wearable and highly sensitive graphene strain sensor for precise home-based pulse wave monitoring," *ACS Sensors*, vol. 2, no. 7, pp. 967–974, Jul. 28, 2017.

[30] A. Nozariasbmarz *et al.*, "Review of wearable thermoelectric energy harvesting: From body temperature to electronic systems," *Appl. Energy*, vol. 258, Jan. 2020, Art. no. 114069.

[31] Y. Wang, Y. G. Shi, D. Q. Mei, and Z. C. Chen, "Wearable thermoelectric generator to harvest body heat for powering a miniaturized accelerometer," *Appl. Energy*, vol. 215, pp. 690–698, Apr. 2018.

[32] W. Peng and H. Wu, "Flexible and stretchable photonic sensors based on modulation of light transmission," *Adv. Opt. Mat.*, vol. 7, no. 12, 2019, Art. no. 1900329.

[33] B. Z. Tian *et al.*, "Coaxial silicon nanowires as solar cells and nanoelectronic power sources," *Nature*, vol. 449, no. 7164, pp. 885–U8, Oct. 2007.

[34] A. S. Dahiya, F. Morini, S. Boubenia, K. Nadaud, D. Alquier, and G. Poulin-Vittrant, "Organic/inorganic hybrid stretchable piezoelectric nanogenerators for self-powered wearable electronics," *Adv. Mat. Technol.*, vol. 3, no. 2, 2018, Art. no. 1700249.

[35] Y. M. Liu *et al.*, "Skin-integrated graphene-embedded lead zirconate titanate rubber for energy harvesting and mechanical sensing," *Adv. Mat. Technol.*, vol. 4, 2019, Art. no. 1900744.

[36] R. S. Yang, Y. Qin, L. M. Dai, and Z. L. Wang, "Power generation with laterally packaged piezoelectric fine wires," *Nature Nanotechnol.*, vol. 4, no. 1, pp. 34–39, Jan. 2009.

[37] K. Zhang, X. Wang, Y. Yang, and Z. L. Wang, "Hybridized electromagnetic–triboelectric nanogenerator for scavenging biomechanical energy for sustainably powering wearable electronics," *ACS Nano*, vol. 9, no. 4, pp. 3521–3529, Apr. 28, 2015.

[38] F.-R. Fan, Z.-Q. Tian, and Z. Lin Wang, "Flexible triboelectric generator," *Nano Energy*, vol. 1, no. 2, pp. 328–334, Mar. 1, 2012.

[39] F. R. Fan, W. Tang, and Z. L. Wang, "Flexible nanogenerators for energy harvesting and self-powered electronics," *Adv. Mat.*, vol. 28, no. 22, pp. 4283–4305, 2016.

[40] Q. Zheng, B. Shi, Z. Li, and Z. L. Wang, "Recent progress on piezoelectric and triboelectric energy harvesters in biomedical systems," *Adv. Sci.*, vol. 4, no. 7, 2017, Art. no. 1700029.

[41] M. M. Apodaca, P. J. Wesson, K. J. M. Bishop, M. A. Ratner, and B. A. Grzybowski, "Contact electrification between identical materials," *Angewandte Chemie-Int. Ed.*, vol. 49, no. 5, pp. 946–949, 2010.

[42] C. Xu *et al.*, "Contact-electrification between two identical materials: Curvature effect,"" *Acs Nano*, Article vol. 13, no. 2, pp. 2034-"2041, Feb. 2019.

[43] L. C. Rome, L. Flynn, E. M. Goldman, and T. D. Yoo, "Generating electricity while walking with loads," *Sci.*, vol. 309, no. 5741, pp. 1725–1728, Sep. 2005.

[44] J. M. Donelan, Q. Li, V. Naing, J. A. Hoffer, D. J. Weber, and A. D. Kuo, "Biomechanical energy harvesting: Generating electricity during walking with minimal user effort," *Sci.*, vol. 319, no. 5864, pp. 807–810, Feb 2008.

[45] K. Yao *et al.*, "Mechanics designs-performance relationships in epidermal triboelectric nanogenerators," *Nano Energy*, vol. 76, Oct. 1, 2020, Art. no. 105017.

[46] Y.-C. Lai *et al.*, "Electric Eel-skin-inspired mechanically durable and super-stretchable nanogenerator for deformable power source and fully autonomous conformable electronic-skin applications," *Adv. Mat.*, vol. 28, no. 45, pp. 10024–10032, 2016.

[47] M. S. Rasel *et al.*, "An impedance tunable and highly efficient triboelectric nanogenerator for large-scale, ultra-sensitive pressure sensing applications," *Nano Energy*, vol. 49, pp. 603–613, Jul. 1, 2018.

[48] H. Chu, H. Jang, Y. Lee, Y. Chae, and J.-H. Ahn, "Conformal, graphene-based triboelectric nanogenerator for self-powered wearable electronics," *Nano Energy*, vol. 27, pp. 298–305, Sep. 1, 2016.

[49] C. He *et al.*, "Hourglass triboelectric nanogenerator as a "direct current" power source," *Adv. Energy Mat.*, vol. 7, no. 19, 2017, Art. no. 1700644.

[50] Z. L. Wang, "Triboelectric nanogenerators as new energy technology for self-powered systems and as active mechanical and chemical sensors," *ACS Nano*, vol. 7, no. 11, pp. 9533–9557, Nov. 26, 2013.

[51] U. Eduok, O. Faye, and J. Szpunar, "Recent developments and applications of protective silicone coatings: A review of PDMS functional materials," *Progress Organic Coatings*, vol. 111, pp. 124–163, Oct. 1, 2017.

[52] S. Niu and Z. L. Wang, "Theoretical systems of triboelectric nanogenerators," *Nano Energy*, vol. 14, pp. 161–192, May 1, 2015.

[53] R. D. I. G. Dharmasena, J. H. B. Deane, and S. R. P. Silva, "Nature of power generation and output optimization criteria for triboelectric nanogenerators," *Adv. Energy Mat.*, vol. 8, no. 31, 2018, Art. no. 1802190.

[54] N. Cui *et al.*, "Dynamic behavior of the triboelectric charges and structural optimization of the friction layer for a triboelectric nanogenerator," *ACS Nano*, vol. 10, no. 6, pp. 6131–6138, Jun. 28, 2016.